THE JOURNAL OF BIOLOGICAL CHEMISTRY
Vol. 278, No. 10, Issue of March 7, pp. 8501–8507, 2003

Printed in U.S.A.

Crystal Structure of GRIP1 PDZ6-Peptide Complex Reveals the Structural Basis for Class II PDZ Target Recognition and PDZ Domain-mediated Multimerization*

Received for publication, December 3, 2002, and in revised form, December 18, 2002
Published, JBC Papers in Press, December 18, 2002, DOI 10.1074/jbc.M212263200

Young Jun Im‡§, Seong Ho Park‡§, Seong-Hwan Rho‡, Jun Hyuck Lee‡, Gil Bu Kang‡, Morgan Sheng¶, Eunjoon Kim‖, and Soo Hyun Eom‡**

From the ‡Department of Life Science, Kwangju Institute of Science and Technology, Gwangju 500-712, South Korea, the ‖Department of Biological Sciences, Korea Advanced Institute of Science and Technology, Daejeon 305-701, South Korea, and the ¶Picower Center for Learning and Memory and the Howard Hughes Medical Institute, Massachusetts Institute of Technology, Cambridge, Massachusetts 02139

PDZ domains bind to short segments within target proteins in a sequence-specific fashion. Glutamate receptor-interacting protein (GRIP)/ABP family proteins contain six to seven PDZ domains and interact via the sixth PDZ domain (class II) with the C termini of various proteins including liprin-α. In addition the PDZ456 domain mediates the formation of homo- and heteromultimers of GRIP proteins. To better understand the structural basis of peptide recognition by a class II PDZ domain and PDZ-mediated multimerization, we determined the crystal structures of the GRIP1 PDZ6 domain alone and in complex with a synthetic C-terminal octapeptide of human liprin-α at resolutions of 1.5 and 1.8 Å, respectively. Remarkably, unlike other class II PDZ domains, Ile-736 at αB5 rather than conserved Leu-732 at αB1 makes a direct hydrophobic contact with the side chain of the Tyr at the −2 position of the ligand. Moreover, the peptide-bound structure of PDZ6 shows a slight reorientation of helix αB, indicating that the second hydrophobic pocket undergoes a conformational adaptation to accommodate the bulkiness of the Tyr side chain, and forms an antiparallel dimer through an interface located at a site distal to the peptide-binding groove. This configuration may enable formation of GRIP multimers and efficient clustering of GRIP-binding proteins.

Synaptic localization and clustering of ion channels and receptors is often mediated by scaffolding molecules containing the protein-protein interaction motifs called PDZ (Postsynaptic density-95/Discs large/Zona occludens-1) domains (1). One of the most abundant molecular recognition elements, these globular domains each contain two α-helices and six β-strands. They usually bind selectively to the C terminus or a short internal segment of interacting proteins (1) and are categorized into four classes according to their specificity for the C-terminal target sequences (2). Class I PDZ domains bind to a C-terminal motif with the sequence *X*-Ser/Thr-*X*-Val/Leu-COOH, where *X* represents any residue, while class II PDZ domains prefer *X*-Φ-*X*-Φ-COOH, where Φ is usually a large hydrophobic residue. Both class I and II domains have a preference for a hydrophobic residue at the 0 position of the ligand. Class III PDZ domains prefer the sequence *X*-Asp-*X*-Val-COOH in which a negatively charged amino acid is at the −2 position (3), while class IV domains prefer the sequence *X*-Ψ-Asp/Glu-COOH in which an acidic residue is at the C-terminal position and where Ψ represents an aromatic residue (4). In addition, there are other classes of PDZ domains that do not fall into any of the aforementioned classes (5, 6), and there are minor discrepancies in the proposed classifications of PDZ domains (7, 8).

Members of the GRIP[1] family proteins (GRIP1 and GRIP2/ABP) contain six to seven PDZ domains (9, 10, 11). GRIP PDZ45, which is classified as a class II PDZ domain (1), binds to the C terminus of the GluR2/3 subunit of AMPA glutamate receptors (9, 10, 12), while GRIP PDZ6, also a class II PDZ domain, interacts with the C terminus of ephrin-B1 ligand and EphB2/EphA7 receptor tyrosine kinases (13, 14, 15). GRIP PDZ6 also interacts with the C terminus of the liprin-α family of multidomain proteins (16), which interact with the leukocyte antigen-related protein family of receptor tyrosine phosphatases (17, 18). Interestingly, the PDZ456 region also reportedly mediates homo- and heteromultimerization of GRIPs (11), suggesting that the PDZ domain is a module mediating multimerization as well as peptide recognition.

The first reported crystal structure of a class II PDZ domain (from hCASK) revealed the presence of a second hydrophobic pocket not seen in class I PDZ domain (19). In addition, this study showed that hCASK PDZ forms a homotetramer by binding to the truncated C-terminal tail of a neighboring PDZ domain that partially mimics the specific peptide ligand, though the self-associated structure does not faithfully represent the actual binding mode of class II PDZ domains due to differences in the amino acid sequences of the true target peptides and the truncated C-terminal tail (19). Another structure of a class II PDZ domain in InaD revealed its association with the −1 position of the ligand via a distinctive intermolecular disulfide bond (20), which is not a canonical non-covalent peptide-PDZ interaction.

To better understand the structural basis of peptide recog-

* This work was supported by grants from the K-JIST project, the Brain Korea 21 Project and Critical Technology 21 (Neurobiology Research Center). The costs of publication of this article were defrayed in part by the payment of page charges. This article must therefore be hereby marked "*advertisement*" in accordance with 18 U.S.C. Section 1734 solely to indicate this fact.

The atomic coordinates and structure factors (code 1N7E and 1N7F.) have been deposited in the Protein Data Bank, Research Collaboratory for Structural Bioinformatics, Rutgers University, New Brunswick, NJ (http://www.rcsb.org/).

§ These authors contributed equally to this work.

** To whom correspondence should be addressed. Tel.: 82-62-970-2549; Fax: 82-62-970-2548; E-mail: eom@kjist.ac.kr.

[1] The abbreviations used are: GRIP, glutamate receptor-interacting protein; ABP, AMPA receptor-binding protein; AMPA, α-amino-3-hydroxy-5-methyl-4-isoxazole-propionic acid; MAD, multiwavelength anomalous dispersion; r.m.s.d., root-mean square deviation.

TABLE I
Data collection and refinement statistics

Data set	Peptide-free (Br-MAD)[a]			Peptide-free	Complex
Crystal form	$P6_522$			$P6_522$	R32
X-ray source	NSLS X8C			NSLS X8C	PF18B
Wavelength	λ 1	λ 2	λ 3	0.900	1.000
	0.9202	0.9192	0.900		
Resolution (Å)	34.5–1.9	34.5–1.9	34.5–1.9	15–1.5	15–1.8
R_{sym}[b] (%)	5.5 (17.4)	5.3 (17.9)	5.3 (13.8)	4.5 (36.0)	8.8 (56.6)
Data coverage total/final shell (%)	98.8/89.1	99.0/91.9	99.7/98.7	98.3/93.3	99.6/97.3
Phasing (34.5–1.9 Å)	0.52 (SOLVE)				
Overall figure of merit refinement					
Resolution (Å)				15–1.5	15–1.8
R_{cryst}[c] total (%)				25.4	20.1
R_{free}[d] total (%)				27.8	22.2
R.m.s. bond length (Å)				1.20	1.26
R.m.s. bond angle (°)				0.005	0.005
Average B vale (Å^2)				25.2	29.4

[a] Derivatized by soaking in the reservoir solution containing 1 M NaBr for 30 s.
[b] $R_{sym} = \Sigma \mid \langle I \rangle - I \mid / \Sigma \langle I \rangle$.
[c] $R_{cryst} = \Sigma \mid \mid F_o \mid - \mid F_c \mid \mid / \Sigma \mid F_o \mid$.
[d] R_{free} calculated with 10% of all reflections excluded from refinement stages using high resolution data.

nition by class II PDZ domains and the mechanisms underlying PDZ-mediated GRIP multimerization, we determined the crystal structures of the GRIP1 PDZ6 domain alone and in complex with a synthetic C-terminal octapeptide of liprin-α1 at resolutions of 1.8 and 1.5 Å, respectively. This is the first description of the crystal structure of a class II PDZ domain non-covalently complexed with its specific peptide ligand, showing an additional role of PDZ domains in the multimerization of PDZ-containing proteins.

EXPERIMENTAL PROCEDURES

Protein Purification and Crystallization—Recombinant GRIP1 PDZ6 (residues 665–761) from *Rattus novergicus* with a cleavable glutathione *S*-transferase tag was expressed in BL21(DE3) *Escherichia coli*, cleaved, purified, and crystallized as previously described (21). The C-terminal octapeptide (ATVRTYSC) of the human liprin-α1 used for PDZ-peptide cocrystallization was chemically synthesized.

Site-directed Mutagenesis and Mutant Protein Preparation—The mutants Y671D and R718D were obtained by site-directed mutagenesis of the plasmid carrying the *GRIP-PDZ6* gene using the QuikChange mutagenesis kit from Invitrogen. The expression and purification of the mutants were done by same procedures with the wild type protein.

Data Collection—A native data set was collected from a peptide-free frozen crystal to 1.5 Å resolution using an ADSC Quantum 4R CCD detector at beamline X8C in the National Synchrotron Light Source. Since bromine is a convenient anomalous scatterer for MAD phasing, a bromine MAD data set was collected from a single crystal soaked for 30 s in cryoprotection solution containing 1 M NaBr (22). A data set was collected from a PDZ-peptide complex to 1.8 Å Bragg spacing using an ADSC Quantum 4R CCD detector at beamline BL-18B at Photon Factory, Tsukuba, Japan.

Structure Determination and Refinement—The structure of the peptide-free PDZ6 domain was determined by MAD using bromine as an anomalous scatterer. The positions of three bromines in the asymmetric unit were located and refined using the program SOLVE (23). The initial phases (overall figure of merit, 0.51) were improved by solvent flattening using the program DM (24). The resultant map was readily interpretable, and model building proceeded using the program O (25), after which the initial model was refined using the program CNS (26). When the crystallographic *R* value for the model was 28.3%, the coordinates were used in the refinement procedures against the 1.5-Å native data set. The final crystallographic *R* value for the peptide-free PDZ6 model using data from 15 to 1.5 Å was 25.4% (R_{free} = 27.8%).

The structure of the PDZ6-octapeptide complex was determined using standard molecular replacement methods using the structure of peptide-free PDZ6 as a starting model. There were two PDZ6 domains related by NCS in the asymmetric unit. After applying a simulated annealing procedure using data to 1.8 Å, the location of the two bound peptides was determined from a $f_o - f_c$ difference electron density map. Densities of all eight residues of the peptide were obvious, indicating they were well ordered within the structure. The octapeptide was modeled using the program O, and the peptide-bound PDZ6 domain was refined to a final crystallographic *R* value of 20.0% and a free *R* value of 22.2%. The refined model of the peptide-bound PDZ6 domain consisted of a PDZ domain dimer (Ala-668-Gln-753) related by 2-fold NCS, two octapeptides, and 240 water molecules. Because of disorder, the N-terminal three and C-terminal eight residues were not modeled. The stereochemistry of the model was analyzed with PROCHECK (27); no residues were found in the disallowed regions of the Ramachandran plot. Data collection and refinement statistics are summarized in Table I. The coordinates and structure factors of PDZ6 and peptide-PDZ6 complex have been deposited with the Protein Data Bank accession numbers 1N7E and 1N7F, respectively.

RESULTS AND DISCUSSION

Overall Structure of the GRIP PDZ6 Domain—GRIP1 PDZ6 is a compact, globular domain containing eight segments of secondary structure: six β-strands that form an antiparallel β-barrel and two α-helices (Fig. 1*A*). Within the crystal structure of the PDZ6-peptide complex, all eight amino acid residues of the peptide ligand were well defined, as shown by the difference electron density map calculated without inclusion of the peptide (Fig. 1*B*), and the strong electron density indicates that the octapeptide was highly ordered. As is typical of most PDZ complexes, the ligand was positioned in the groove between the βB strand and the αB helix, oriented anti-parallel to βB as an additional strand. In addition, the carboxylate-binding loop contained a PLGI sequence (residues 681–684), often referred to as the "GLGF motif."

GRIP1 PDZ6 binds to the liprin-α C-terminal TYSC sequence (*X*-Φ-*X*-Φ-COOH) via a class II hydrophobic PDZ interaction; it contains two hydrophobic pockets that can accommodate bulky hydrophobic residues at the 0 and −2 positions of the ligand. In the peptide-bound state, PDZ6 domain forms an antiparallel dimer in an asymmetric unit of the crystallized complex, whereas peptide-free PDZ6 forms a similar dimer through a crystallographic 2-fold axis in its crystal. As was seen in the crystal structures of the hCASK and NHERF PDZ domains, the peptide binding pocket of peptide-free PDZ6 is occupied by the C-terminal end (PASS-COOH) of a neighboring molecule mimicking the recognition of the peptide ligand (19, 28). Superposition of the crystal structures of the peptide-free and peptide-bound PDZ6 domains shows a slight shift in the αB helix, which widens the peptide binding pocket and enables accommodation of the bulky side chain of tyrosine from the ligand. The free and peptide-bound structures of the PDZ6 domain showed an α-carbon root-mean square deviation (r.m.s.d.) of 1.1 Å when the six structurally conserved β-strands

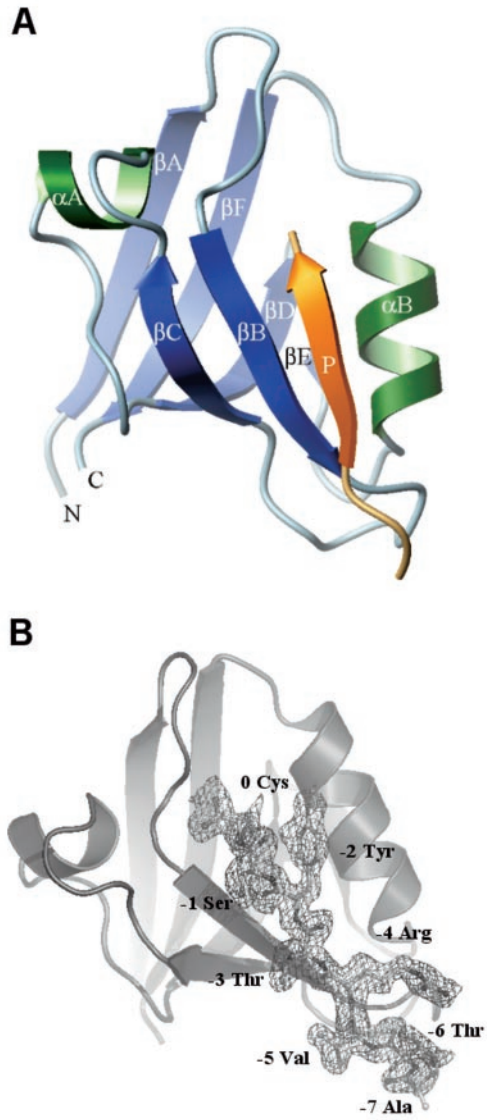

FIG. 1. **Structure of the GRIP1 PDZ6 domain.** *A*, ribbon diagram showing the overall structure of the GRIP1 PDZ6-peptide complex. The β-strands are labeled as βA-βF, and the α-helices are labeled αA and αB. The peptide (*orange*) inserts between the βB strand and the αB helix and forms an antiparallel β-sheet with βB. This picture was drawn using MolMol (33). *B*, quality of the peptide electron density map. An omit map was calculated using coefficients of $F_o - F_c$ at 1.8 Å resolution, where F_c is the calculated structure factor from the PDZ6-peptide complex with the peptide removed. The map, contoured at 3σ, defines the peptide carboxylate group and all eight peptide residues. This figure was made using PyMOL (available on the web at www.pymol.org).

were used for the superposition. With an r.m.s.d. of 1.57 Å for the residues spanning positions 732–742, helix αB showed the highest structural variance among secondary elements.

Molecular Basis of Peptide Recognition—Because the amino acid sequence of the rat GRIP1 PDZ6 domain used in this study is identical to human GRIP1 PDZ6, we used a synthetic octapeptide (ATVRTYSC) that mimics the C terminus of human liprin-α1 as a ligand. The last five residues of liprin-α are identical among known isoforms, and the residues at the 0 and −2 positions are well conserved as compared with those from other known PDZ6 binding partners, *e.g.* EphB2 receptor (Fig. 2*B*). The C terminus of the ligand binds as an additional strand to the anti-parallel β-sheet of the PDZ domain and makes hydrophobic contacts with helix αB, while the peptide backbone of the C-terminal four residues is anchored to strand βB by hydrogen bonds.

Despite variations in the sequences of many PDZ domains, their carboxylate-binding loops are highly conserved in terms of overall structure and the hydrogen-bonding pattern to the ligand carboxylate group. The C-terminal carboxylate group of our octapeptide formed hydrogen bonds with the backbone amide groups of Leu-682, Gly-683, and Ile-684 in the carboxylate-binding loop, and was within hydrogen-bonding distance of two fully occupied water molecules (Fig. 3*A*).

The amino acid residues at ligand positions 0 and −2 are key to the specific recognition by the PDZ domain. The side chain of Cys-0 is situated at the center of the first hydrophobic cavity, which is composed of Leu-682, Ile-684, Ile-686, and Leu-739 (Fig. 3*B*) and is of sufficient size to accommodate various hydrophobic side chains ranging from those of Ala to Phe, but not hydrophilic residues.

The second hydrophobic pocket, which accommodates the Tyr residue at ligand position −2, is composed of Ile-686 from the βB strand and Ile-736 and Ile-739 from helix αB. Within the structures of previously described class I and class II PDZ domains, the residue at ligand position −2 usually binds to the side chain of a residue located at the N-terminal end of helix αB (position αB1) of the PDZ (7, 29). In class I PDZ domains, serine or threonine at the −2 position forms hydrogen bonds with the side chain of a polar residue at the start of the αB helix. In class II PDZ domains, the corresponding residue at the αB1 position is highly conserved (mostly hydrophobic) and considered to be critical for determining the specificity of ligand binding. In hCASK PDZ, for example, Val at αB1 recognizes the residue at ligand position −2 (19). Another known class II PDZ domain, the crystal structure of InaD, showed that the Cβ and Cγ atoms of Glu at αB1 take part in the hydrophobic interactions with Phe at the ligand −2 position (20).

Within the structure of the GRIP1 PDZ6-peptide complex, by contrast, the side chain of Tyr-2 did not make a direct contact with the conserved Leu-732 at αB1. Instead, the Tyr aromatic ring was oriented toward the first hydrophobic cavity and stacked with the side chain of Ile-736 located at second turn of the helix αB (position αB5). Still, Leu-732 appeared to indirectly contribute to the ligand binding by offering the hydrophobic environment necessary accommodate a bulky hydrophobic residue at ligand position −2. This finding suggests a novel mode of peptide recognition in which a hydrophobic residue at the αB5 position can supersede the role of the conserved hydrophobic residue at the αB1 position in class II PDZ domains.

Interestingly, superposition of peptide-free and peptide-bound structures showed that a slight reorientation of the αB helix occurs to accommodate the side chain of Tyr-2 (Fig. 3*C*). The B-factor plots of the structures showed helix αB to have the highest B values among the secondary structure elements in both the peptide-free and peptide-bound structures. Gly-743, which is located in the βF-αB loop, adjacent to Ala-742 in the C-terminal end of helix αB, exhibited the largest positional shift upon peptide binding. The resultant shift in the C-terminal end of helix αB enlarged the second hydrophobic pocket, suggesting that Gly-743 plays a key role in the conformational adaptation of helix αB by providing geometrical freedom to the preceding residues. In addition, a positional shift of 1.25 Å in the Cβ atom of Leu-736 at αB5, which interacts with ligand Tyr-2 likely avoids steric hindrance due to the bulkiness of the Tyr side chain (Fig. 3*D*). Supporting this view, the four peptide backbone positions of the ligand PASS-COOH in the self-associated structure and TYSC in the PDZ-peptide complex were identical in both structures; however, there was a positional difference of 1.25 Å in the Cβ atom of Leu-736, which interacts with Tyr-2, due to the difference of the bulkiness of the side chain at that position (Fig. 3*D*). Thus, the shift of helix αB is

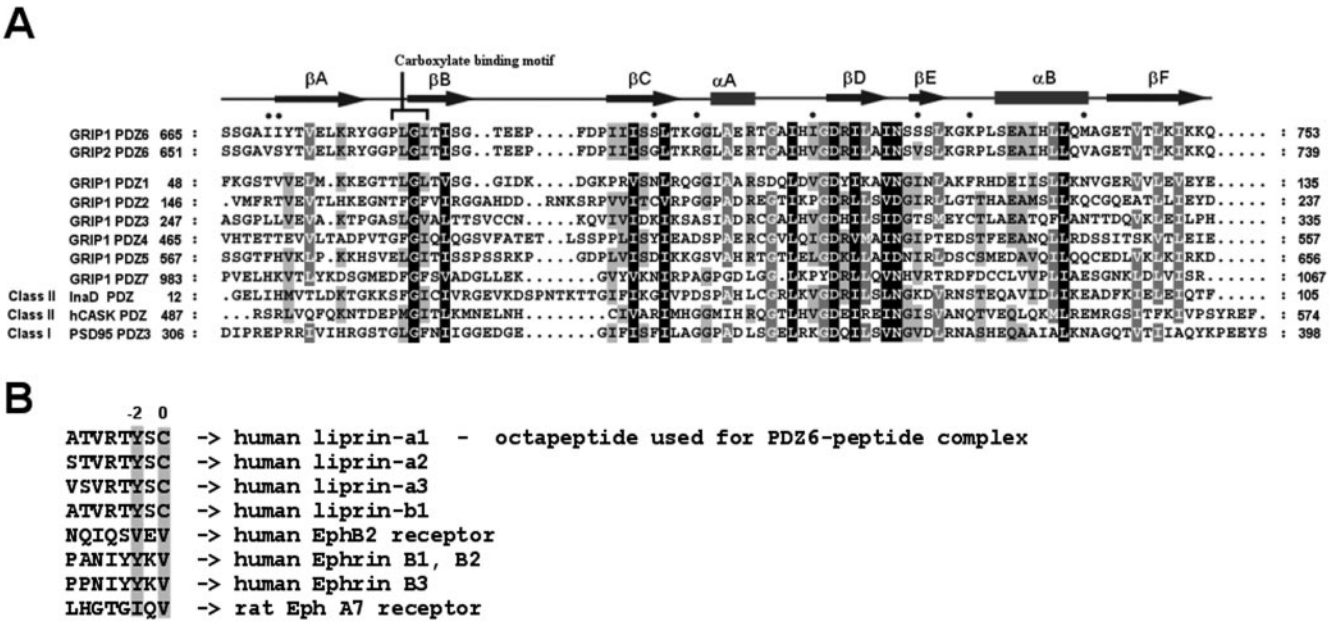

FIG. 2. **Sequence alignment of selected PDZ domains.** *A*, the amino acid sequences of the indicated PDZ domains from rat GRIP1, rat GRIP2, *Drosophila* InaD, human CASK, and rat PSD95 were aligned using the program ClustalX (32). Highly conserved residues are shaded in *black* and *gray*. The secondary structure elements of GRIP1 PDZ6 are shown as *arrows* (β-sheet), *bars* (α helix), and *lines* (connecting loops). The variant residues within the PDZ6 domains of GRIP1 and GRIP2 are indicated with *black dots*. *B*, several known ligands of the GRIP PDZ6 domain. Only the C-terminal eight residues of each ligands are shown. The sequence of the octapeptide used for the PDZ6-peptide complex examined here is indicated with an *asterisk*.

determined by the difference in the size of the residue at ligand position −2. This structural flexibility may explain the ability of GRIP1 PDZ6 to bind various target peptides with different hydrophobic amino acids at the −2 position (Fig. 2*B*).

Within the structure of the PDZ6-peptide complex, ligand residues at the −1 and −3 positions also appear to contribute to its recognition. Ser-1 hydrogen bonds with Thr-685 in the βB strand in one protomer of the dimer, while Thr-3 hydrogen bonds with Ser-687 in the other protomer. The residues at the −3 position of known PDZ6 ligands are highly conserved and all contain hydroxyl groups (Fig. 2*B*), implying direct contribution to the specificity and affinity for the GRIP1 PDZ6 domain. The side chain of Arg at ligand position −4 also participates in water-mediated hydrogen bonding with Glu-690 at the terminus of the βB strand. Although there is no conserved pattern of interaction at the −1, −3, and −4 positions among PDZ domains, it likely fine tunes the specificity of PDZ-ligand recognition.

Dimerization of PDZ6 Domains—PDZ domain-mediated multimerization is a common feature for a number of PDZ domain proteins. Such multimerization of *Drosophila* InaD, which is mediated by its PDZ3 or PDZ4 domain, does not disturb the binding of target proteins (30) nor does oligomerization of NHERF/EBP50, which is mediated by its two PDZ domains (31). Unfortunately, these studies provide no structural evidence for the mechanism of multimerization or why it does not affect ligand binding. At present, the structures of InaD PDZ3 or PDZ4 remain unknown, and the crystal structures of the NHERF PDZ1 domains provide no clues (28, 29).

GRIP/ABP proteins reportedly form homo- or heteromultimers through their PDZ456 domains (11). Although it is not known how these three PDZ domains mediate multimer formation, our preliminary results from size exclusion chromatography, and dynamic light-scattering experiments indicate that GRIP1 PDZ6 forms a dimer whether free or complexed, which suggests that GRIP1 PDZ6, itself, has the ability to mediate dimer formation. Consistent with that idea, the crystal structure of peptide-bound GRIP1 PDZ6 showed formation of a tightly associated PDZ6 dimer related by a non-crystallographic 2-fold axis in the asymmetric unit (Fig. 4*A*). The dimeric interface between the two PDZ domains involves a βA strand and an αA-βD loop from each protomer; the βA strands form anti-parallel β-sheets around the center of the 2-fold axis, with the N and C termini of each PDZ domain pointing in opposite directions. The peptide binding pockets were located at the distal sides of the dimeric interface, situated in anti-parallel fashion, which enabled spatially independent binding of target ligands. This dimeric interaction was supported by six hydrogen bonds between the two anti-parallel βA strands and hydrophobic forces between non-polar atoms in the interface. The amount of surface area buried upon dimer formation is 619.0 Å^2, or 12.3% of the total surface area of each monomer. Such independent target binding by PDZ multimers was also detected with InaD and NHERF proteins using biochemical analyses (30, 31).

In the peptide-free crystal structure with the space group $P6_522$, there was one molecule in the asymmetric unit. However, the same dimeric interaction described above was observed via a crystallographic 2-fold axis. It is possible that the dimer in the solution can arrange into a crystallographic symmetry axis in a different crystallographic environment because it shows little difference of the r.m.s.d. for all Cα atoms (0.6 Å) between the two protomers in the asymmetric unit of a peptide-bound crystal. Another intermolecular interaction with a symmetry-related molecule in the peptide-free crystal structure is the association through C-terminal exchange into the ligand binding pockets between two monomers (Fig. 4*B*). In this case C termini serve as ligands for neighboring PDZ molecules, which is reminiscent of the crystal structures of NHERF PDZ1 and hCASK PDZ domains (19, 28). However, the C-terminal amino acid sequence of the PDZ6 construct (PASS-COOH) differs from the usual class II PDZ target peptides (*X*-Phe/Tyr-*X*-Phe/Val/Ala-COOH). The backbone atoms of the C-terminal four residues of the neighboring molecule, located in the ligand-binding groove, shows little positional difference from the location C-terminal octapeptide of liprin-α1 complexed with the

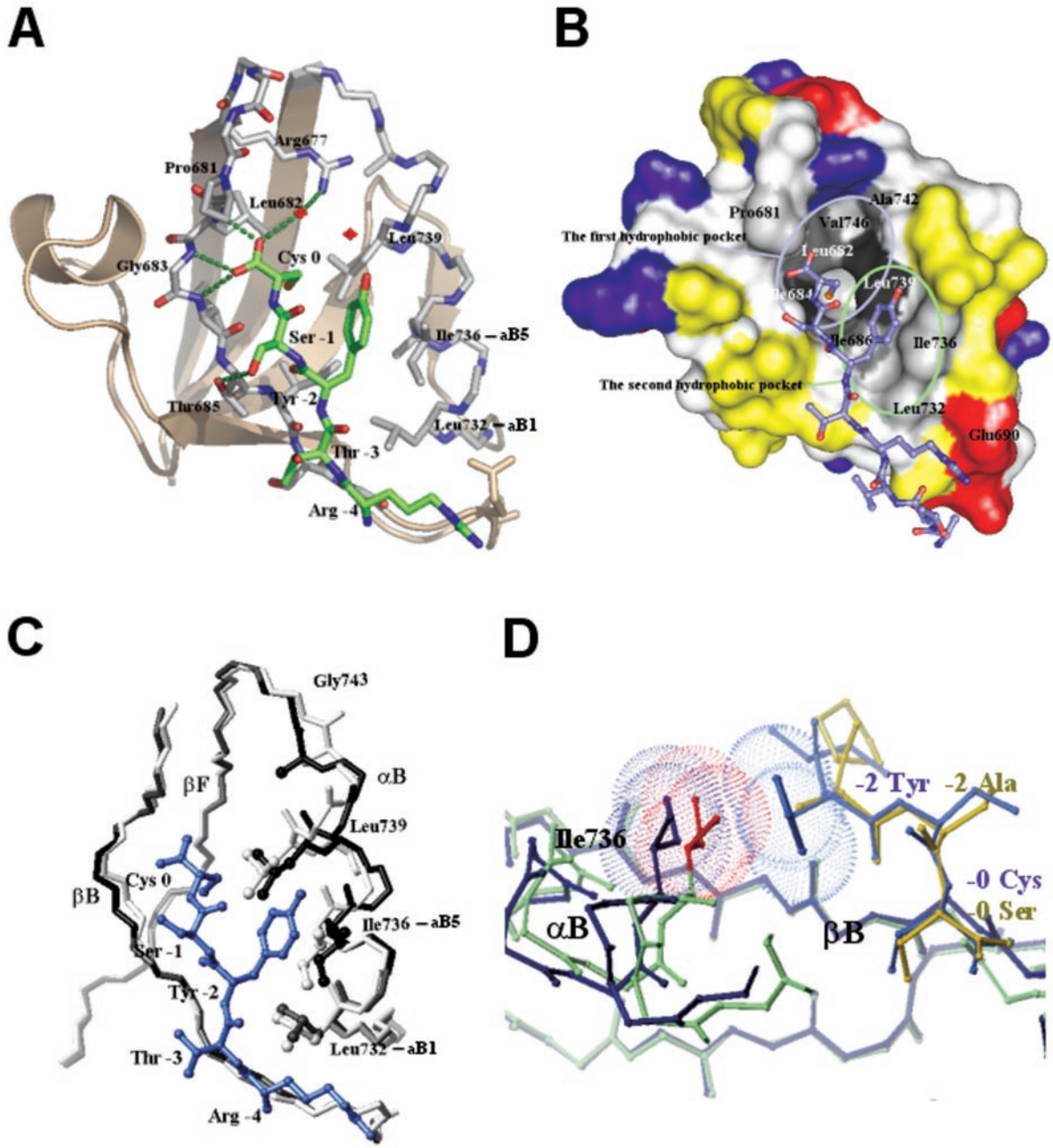

FIG. 3. **The peptide-binding site.** *A*, ball and stick model of the peptide binding pocket and its specific ligand (ATVRTYSC). Only the last four residues of the peptide are shown (*green*), and for clarity only side chains of the residues involved in the peptide binding are shown. *Dashed lines* represent hydrogen bonds around the carboxylate binding site. A water molecule, shown as a *red ball*, forms a hydrogen bond with one of the ligand C-terminal carboxylic oxygen atoms. The majority of the hydrogen bonds are between the peptide backbone and the carboxylate-binding loop or strand βB. *B*, molecular surfaces of GRIP PDZ6 showing the hydrophobic binding pocket and the bound peptide. The hydrophobic residues are colored *white*, and the hydrophobic side chains within the binding pocket are colored in *gray scale*. The polar, acidic, and basic residues are colored *yellow*, *red*, and *blue* respectively. The two hydrophobic binding pockets are indicated by *circles*. The side chains of hydrophobic ligand residues Cys-0 and Try-1 dip into the hydrophobic binding pockets. *C*, conformational changes upon peptide binding. Superposition of the peptide-free and peptide-bound structures was done using the six β-strands, which do not undergo conformational change upon peptide binding. The peptide-free and peptide-bound PDZ structures are shown in *white* and *gray*, respectively. The segments that undergo large conformational changes upon peptide binding are colored *black*. *D*, ball and stick model showing a conformational change of Ile-736. Peptide-bound PDZ6 is colored *dark blue*; self-associated PDZ6 is colored *green*. The peptide ligand and C-terminal tail of the PDZ6 construct are colored *pale blue* and *yellow*, respectively. The bulky hydrophobic side chain of Tyr-2 makes hydrophobic contact with Ile-736.

PDZ6. Apparently, hydrophobic pockets of GRIP1 PDZ6 accommodated smaller hydrophobic residues or the residues that partly mimic a hydrophobic moiety. Most likely, the self-association observed in the peptide-free crystal structure is not dimeric interaction but molecular packing interaction within the crystal lattice. Consistent with this idea, a PDZ6 construct in which the last seven residues (residues 665–754 lacking DAQPASS) were deleted still formed a dimer in solution identified by size exclusion chromatography (data not shown).

To further confirm the presence of PDZ6 dimer in solution, which is shown in Fig. 4*A*, we did mutational analysis on the residues at the dimeric interface and measured the molecular weights of the mutants and wild type PDZ domains in solution using size exclusion chromatography (Fig. 4). The Y671D mutant, which was expected to disrupt the hydrophobic interaction in the dimeric interface, was eluted as a monomer, while

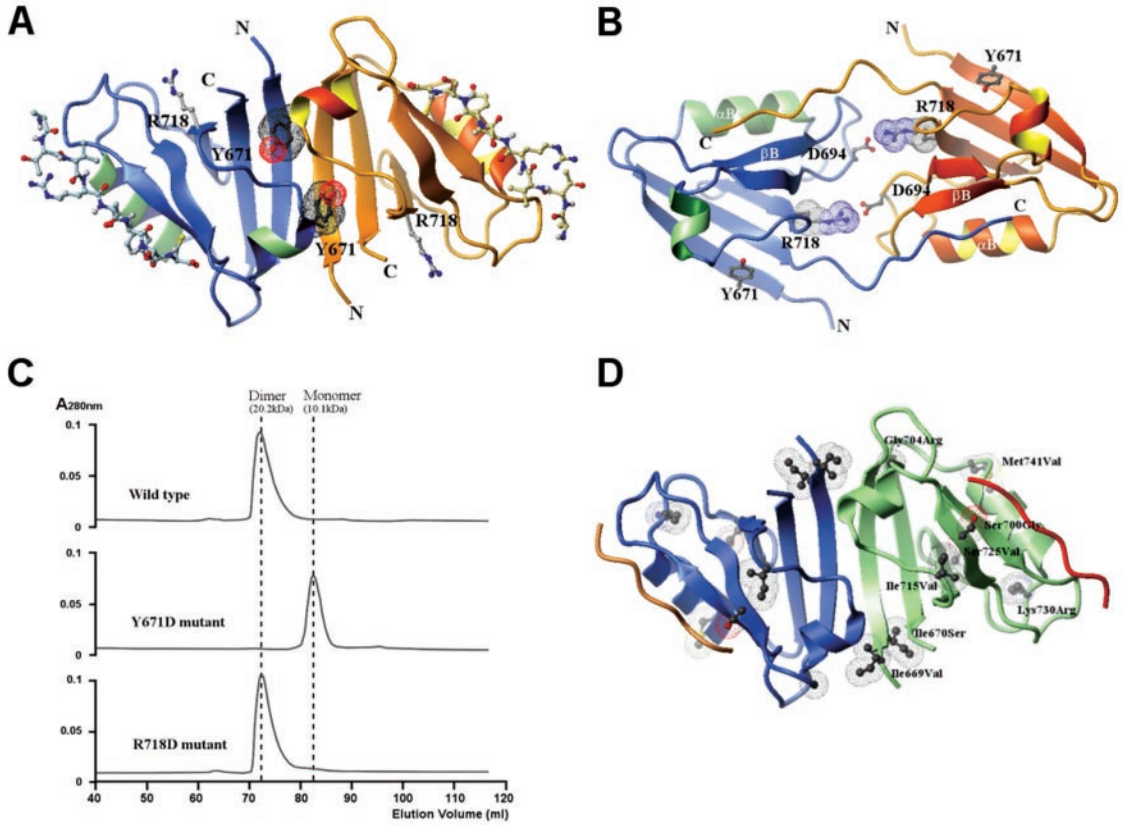

FIG. 4. **Dimerization of GRIP PDZ6.** *A*, dimeric structure of PDZ6 domain. PDZ6 domains form a dimer via interaction of antiparallel βA strands and αA-βD loops. Peptide ligands bound to the opposite side of the PDZ6 dimer are represented in ball-and-stick. *B*, self-association of two GRIP PDZ6 domains related by a 2-fold crystallographic axis was observed in the peptide-free PDZ6 crystal. Each C terminus serves as a ligand for a neighboring PDZ molecule. *C*, effects of mutations on dimerization. Molecular weights of mutants Y671D and R731D and a wild type PDZ domain were estimated by size exclusion chromatography (Superdex 75 HR 16/60 column). The mutated residues, Y671D and R718D, were shown in ball and stick with van der Waals radius in *A* and *B*. The elution profiles of a wild type, Y671D and R718D mutants. This result suggests that the dimer in solution is the form shown in *A*. *D*, the variable residues within the PDZ6 domains of GRIP homologues are represented in ball-and-stick. Only one variable residue, Ile-669, which is Val in GRIP2, is located in the dimeric interface.

the wild type PDZ6 was a dimer in solution (Fig. 4*C*). It indicates that Tyr-671 is located at the dimeric interface and plays an important role in hydrophobic interaction of the interface. However, the disruption of salt-bridge by the mutation R718D on the residue participating in self-association of the domains in the crystalline state did not affect the oligomeric state of the PDZ domains. These results together with the dimerization of peptide-bound PDZ6 in both the crystalline state and in solution strongly suggests that the dimeric structure of PDZ6 shown in Fig. 4*A* is representative of dimeric PDZ6 *in vivo*.

We therefore propose that the GRIP PDZ6 domain plays a crucial role in heteromultimerization of GRIPs. GRIP2, a homolog of GRIP1, has 58% overall amino acid sequence identity with GRIP1, and the two isoforms share 84% identity in the region containing the PDZ456 domains and 91% identity (95% similarity) in the PDZ6 domain. Notably, the residues in the region of the dimeric interface (βA strand and αA-βD loop) are identical except for one conserved change (Ile-669 in GRIP1 and Val-655 in GRIP2) (Fig. 4*C*). Collectively, these findings indicate that GRIP PDZ6 dimers use the same dimeric interface for both homo- and heterodimerization.

In summary, we observed a novel mode of peptide recognition by the class II GRIP PDZ6 domain. Ile-736 at the αB5 position was involved in specific recognition of the ligand, and the conformational adaptation of the αB helix induced by ligand binding accommodated the hydrophobic moiety at ligand position −2. In addition, the dimeric PDZ6 structure described in this study is the first example of a functional role of PDZ domains in multimerization. Formation of antiparallel PDZ6 domain dimers is mediated by an interface located at a site distinct from the peptide-binding groove, resulting in independent target binding by the PDZ multimer. This mechanism could enable efficient clustering of various target proteins though multimerization of GRIP proteins.

Acknowledgments—We thank Professor N. Sakabe and Drs. M. Suzuki and N. Igarashi for kind support in x-ray data collection at beamline BL-18B of Photon Factory, Tsukuba, Japan. We thank Dr. J. Berendzen and L. Flaks for data collection at beamline X8C of National Synchrotron Light Source at Brookhaven National Laboratory. We also thank Dr. H. S. Lee and G. H. Kim at the BL6B of Pohang Accelerator Laboratory, Pohang, Korea.

REFERENCES

1. Sheng, M., and Sala, C. (2001) *Annu. Rev. Neurosci.* **24,** 1–29
2. Songyang, Z., Fanning, A. S., Fu, C., Xu, J., Marfatia, S. M., Chishti, A. H., Crompton, A., Chan, A. C., Anderson, J. M., and Cantley, L. C. (1997) *Science* **275,** 73–77
3. Stricker, N. L., Christopherson, K. S., Yi, B. A., Schatz, P. J., Raab, R. W., Dawes, G., Bassett, D. E. Jr., Bredt, D. S., and Li, M. (1997) *Nat. Biotechnol.* **15,** 336–342
4. Vaccaro, P., Brannetti, B., Montecchi-Palazzi, L., Philipp, S., Citterrich, M. H., Cesareni, G., and Dente, L. (2001) *J. Biol. Chem.* **276,** 42122–42130
5. Maximov, A., Sudhof, T. C., and Bezprozvanny, I. (1999) *J. Biol. Chem.* **274,** 24453–24456
6. Borrell-Pages, M., Fernandez-Larrea, J., Borroto, A., Rojo, F., Baselga, J., and Arribas, J. (2000) *Mol. Biol. Cell* **11,** 4217–4225
7. Bezprozvanny, I., and Maximov, A. (2001) *FEBS Lett.* **509,** 457–462
8. Harris, B. Z., and Lim, W. A. (2001) *J. Cell Sci.* **114,** 3219–3231
9. Srivastava, S., Osten, P., Vilim, F. S., Khatri, L., Inman, G., States, B., Daly, C., DeSouza, S., Abagyan, R., Valtschanoff, J. G., Weinberg, R. J., and Ziff, E. B. (1998) *Neuron* **21,** 581–591
10. Wyszynski, M., Valtschanoff, J. G., Naisbitt, S., Dunah, A. W., Kim, E., Standaert, D. G., Weinberg, R., and Sheng, M. (1999) *J. Neurosci.* **19,** 6528–6537
11. Dong, H., Zhang, P., Song, I., Petralia, R. S., Liao, D., and Huganir, R. L. (1999)

J. Neurosci. **19,** 6930–6941
12. Dong, H., O'Brien, R. J., Fung, E. T., Lanahan, A. A., Worley, P. F., and Huganir, R. L. (1997) *Nature* **386,** 279–284
13. Bruckner, K., Pablo Labrador, J., Scheiffele, P., Herb, A., Seeburg, P. H., and Klein, R. (1999) *Neuron* **22,** 511–524
14. Lin, D., Gish, G. D., Songyang, Z., and Pawson, T. (1999) *J. Biol. Chem.* **274,** 3726–3733
15. Torres, R., Firestein, B. L., Dong, H., Staudinger, J., Olson, E. N., Huganir, R. L., Bredt, D. S., Gale, N. W., and Yancopoulos, G. D. (1998) *Neuron* **21,** 1453–1463
16. Wyszynski, M., Kim, E., Dunah, A. W., Passafaro, M., Valtschanoff, J. G., Serra-Pages, C., Streuli, M., Weinberg, R. J., and Sheng, M. (2002) *Neuron* **34,** 39–52
17. Serra-Pages, C., Kedersha, N. L., Fazikas, L., Medley, Q., Debant, A., and Streuli, M. (1995) *EMBO J.* **14,** 2827–2838
18. Serra-Pages, C., Medley, Q. G., Tang, M., Hart, A., and Streuli, M. (1998) *J. Biol. Chem.* **273,** 15611–15620
19. Daniels, D. L., Cohen, A. R., Anderson, J. M., and Brunger, A. T. (1998) *Nat. Struct. Biol.* ***5***, 317–325
20. Kimple, M. E., Siderovski, D. P., and Sondek, J. (2001) *EMBO J.* **20,** 4414–4422
21. Park, S. H., Im, Y. J., Rho, S. H., Lee, J. H., Yang, S., Kim, E., and Eom, S. H. (2002) *Acta Cryst. D* **58,** 1063–1065
22. Dauter, Z., Dauter, M., and Rajashankar, K. R. (2000) *Acta Cryst. D* **56,** 232–237
23. Terwilliger, T. C., and Berendzen, J. (1999) *Acta Cryst. D* **55,** 1872–1877
24. Collaborative Computational Project, Number 4 (1994) *Acta Cryst. D* **50,** 760–763
25. Jones, T. A., Zou, J-Y., Cowan, S. W., and Kjeldgaard, M. (1991) *Acta Cryst. A* **47,** 110–119
26. Brunger, A. T., Adams, P. D., Clore, G. M., DeLano, W. L., Gros, P., Grosse-Kunstleve, R. W., Jiang, J.-S., Kuszewski, J., Nilges, N., Pannu, N. S., Read, R. J., Rice, L. M., Simonson, T., and Warren, G. L. (1998) *Acta Cryst. D* **54,** 905–921
27. Laskowski, R. A., MacArthur, M. W., Moss, D. S., and Thornton, J. M. (1993) *J. Appl. Crystallogr.* **26,** 283–291
28. Karthikeyan, S., Leung, T., Birrane, G., Webster, G., and Ladias, J. A. A. (2001) *J. Mol. Biol.* **308,** 963–973
29. Karthikeyan, S., Leung, T., and Ladias, J. A. (2001) *J. Biol. Chem.* **276,** 19683–19686
30. Xu, X. Z., Choudhury, A., Li, X., and Montell, C. (1998) *J. Cell Biol.* **142,** 545–555
31. Lau, A. G., and Hall, R. A. (2001) *Biochemistry* **40,** 8572–8580
32. Thompson, J. D., Gibson, T. J., Plewniak, F., Jeanmougin, F., and Higgins, D. G. (1997) *Nucleic Acids Res.* **24,** 4876–4882
33. Koradi, R., Billeter, M., and Wuthrich, K. (1996) *J. Mol. Graphics* **14,** 51–55